Determination of Absolute Orientation of Protein α-Helices at Interfaces Using Phase-Resolved Sum Frequency Generation Spectroscopy

Schmüser, L.; Roeters, S.; Lutz, H.; Woutersen, S.; Bonn, M.; Weidner, T.

DOI
10.1021/acs.jpclett.7b01059

Publication date
2017

Document Version
Final published version

Published in
The Journal of Physical Chemistry Letters

THE JOURNAL OF PHYSICAL CHEMISTRY Letters

Letter

pubs.acs.org/JPCL

Determination of Absolute Orientation of Protein α-Helices at Interfaces Using Phase-Resolved Sum Frequency Generation Spectroscopy

Lars Schmüser,[†] Steven Roeters,[‡] Helmut Lutz,[†] Sander Woutersen,[‡] Mischa Bonn,[†] and Tobias Weidner*[,†,§]

[†]Molecular Spectroscopy Department, Max Planck Institute for Polymer Research, 55128 Mainz, Germany

[‡]Van 't Hoff Institute for Molecular Sciences, University of Amsterdam, 1098 EP Amsterdam, The Netherlands

[§]Department of Chemistry, Aarhus University, 8000 Aarhus C, Denmark

Supporting Information

ABSTRACT: Understanding the structure of proteins at surfaces is key in fields such as biomaterials research, biosensor design, membrane biophysics, and drug design. A particularly important factor is the orientation of proteins when bound to a particular surface. The orientation of the active site of enzymes or protein sensors and the availability of binding pockets within membrane proteins are important design parameters for engineers developing new sensors, surfaces, and drugs. Recently developed methods to probe protein orientation, including immunoessays and mass spectrometry, either lack structural resolution or require harsh experimental conditions. We here report a new method to track the absolute orientation of interfacial proteins using phase-resolved sum frequency generation spectroscopy in combination with molecular dynamics simulations and theoretical spectral calculations. As a model system we have determined the orientation of a helical lysine-leucine peptide at the air−water interface. The data show that the absolute orientation of the helix can be reliably determined even for orientations almost parallel to the surface.

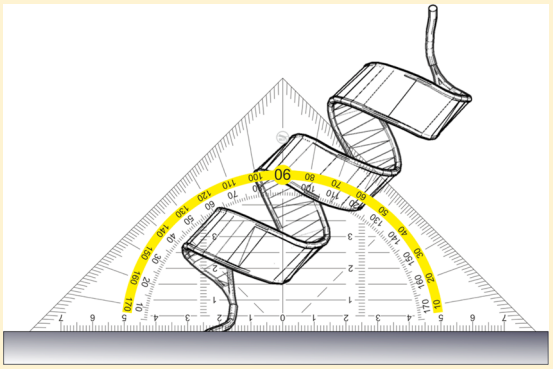

A molecular understanding of the interaction of proteins or peptides with surfaces is essential for the rational design of biomaterials for use in implants and sensors but also for comprehending the interfacial biology at lipid membranes and mineralized tissue.[1−3] An important question for biologists, bioengineers, and pharmacologists is the orientation of proteins when bound to surfaces: Is the enzyme active site within a protein chip pointing toward the solute for effective detection?[4] Which parts of a membrane protein are accessible for interaction with therapeutic drugs?[3] Which sites are in contact with minerals and control the nucleation of hard tissue?[5] Despite the importance, the experimental observation of protein orientation is still challenging. The most established methods are based on enzyme-linked immunoassays,[6,7] where the accessibility of antibody binding sites is observed. While this method provides important practical information for bioengineers, the detail of structural information obtained is limited. Time of flight secondary ion mass spectrometry (ToF-SIMS) has recently been developed to probe protein orientation using its extremely shallow probing depth to detect asymmetries in the amino acid distribution within ordered protein films to determine the molecular orientation.[8] A drawback of ToF-SIMS is that the experiments require ultrahigh vacuum conditions, which makes sample preparation difficult and can alter or destabilize protein structures. Nuclear magnetic resonance[9] and electron paramagnetic relaxation[10] can determine the orientation of proteins but need a series of isotope- and spin-labeled proteins, which are time-consuming, often difficult to produce, and limit the size of proteins that can be studied.

Over the past decade sum frequency generation (SFG) spectroscopy has been developed into a reliable method to probe proteins of arbitrary size at interfaces *in situ* and in real time without the need for labels.[11−13] In an SFG experiment, infrared (IR) and visible laser beams are overlapped in space and time at an interface to generate sum frequency photons by optical frequency mixing.[14] When the IR light is in resonance with a vibrational mode of molecules at the interface, this leads to an enhancement of the SFG process and corresponding features in the resulting spectra. In analogy to IR and Raman spectroscopy, SFG in the amide I region (1600−1700 cm^{-1}) allows the determination of the secondary and tertiary structure of proteins. SFG has been used to determine the structure of proteins on membranes, polymers, self-assembled monolayers,

Received: May 2, 2017
Accepted: June 12, 2017
Published: June 12, 2017

DOI: 10.1021/acs.jpclett.7b01059
J. Phys. Chem. Lett. 2017, 8, 3101−3105

and inorganic surfaces.[11,15−17] Reliable protocols have been developed to determine secondary structures and tilt angles of entire proteins or individual protein sites[18] with respect to the surface.

However, published methods for determining the orientation of protein backbones are based on homodyne SFG intensity spectra[19−21] and as such are unable to tell the *absolute* orientation of the protein, pointing "up" or "down", relative to the surface. As discussed above, for applications the absolute orientation is often a key factor. The inability to infer absolute orientations from SFG intensity spectra originates from the fact that the intensity is proportional to the square of the SFG response of the protein ensemble. The SFG response is a complex variable, and in particular the sign of the imaginary part, or, equivalently, the phase of the SFG response, directly reflects the absolute orientation. Oppositely oriented moieties are precisely 180° out of phase. The phase of a signal can be determined by interfering the SFG signal with a reference signal of known phase.

Phase-resolved SFG has been used to determine the chirality, but not orientation, of interfacial proteins.[22−25] It has been used to infer the absolute orientation of small molecules at interfaces, which requires, however, knowledge of the orientation of the molecular hyperpolarizability tensor (the outer product of the transition dipole moment and the transition polarizability) relative to the molecular axis; for methyl, carbonyl, and water molecules,[26−29] this relation is well-known (see the Supporting Information for the orientation of the amide-I transition dipole moment and transition polarizability). However, because of the pluriform nature of proteins, the orientation of the molecular hyperpolarizability tensor of a given normal mode relative to the orientation of the protein is different for each protein, as it is determined by the positions and orientations of the local modes and the couplings between them.[19] In other words, for protein systems, even knowing the phase of the signal does not directly provide absolute orientation information. This requires, in addition, knowledge of the orientation of the hyperpolarizability tensor in the protein molecular frame. Here, we show that for a model protein, combining heterodyne SFG with molecular hyperpolarizability calculations, we can determine the absolute orientation of proteins at an interface.

The experiments were performed with the well-established model peptide LKα14, which is based only on leucine (L) lysine (K) amino acids and an acetylated N-terminus (Ac-LKKLLKLLKKLLKL) and has been designed to adopt an α-helical secondary structure at the air−water interface (see Scheme 1).[30,31]

To determine the molecular hyperpolarizabilty tensors of the amide-I normal modes of LKα14 at the air−water interface, we have first performed molecular dynamics simulations (MD) of the assembly of the peptides at the air−water interface. A snapshot of the MD simulation, taken at 100 ns, is shown in Figure 1a,b. The snapshot illustrates that the peptides assume a mostly α-helical secondary structure at the interface. The hydrophobic leucines point out of the water phase, and the hydrophilic lysines are in contact with the water. This general conformation is in agreement with previously published experimental and theoretical studies of LK peptides at water surfaces and other hydrophobic interfaces.[32−37]

The simulation indicates the peptides are oriented largely parallel to the water surface, in good agreement with previous experimental and theoretical results. However, a more quantitative analysis of the orientation of the peptide backbone and the average amide-I transition dipole moment (TDM) orientation shown in Figure 1c shows that the peptides are not oriented entirely parallel to the water surface (see Experimental Methods and the Supporting Information for more details about the analysis). The amide-I TDM and the long peptide helix axis are tilted, with angles of 80° and 82°, respectively, with respect to the surface normal and the N-termini pointing towards the water phase.

Phase-resolved SFG spectra for a monolayer of LKα14 at the air−water interface are shown in Figure 2: panels a and b display the imaginary and real SFG spectra, respectively. The imaginary spectrum exhibits a pronounced peak near 1630 cm^{-1}. The real spectrum shows the related zero crossing close to 1630 cm^{-1}.

A convenient way to determine helical peptide orientation from SFG data is to analyze peak ratios obtained from fitted spectra for ssp and ppp polarization combinations. However, at the air−water interface, the ppp combination consists of several hyperpolarizability tensor elements and is underdetermined due to the intrinsic uncertainty of the interfacial refractive index. We therefore chose to directly compare the experimental SFG data with the simulation, by calculating theoretical imaginary and real SFG spectra from the 100 ns MD snapshot shown in Figure 1. This approach also prevents any ambiguities that might arise from peak assignments to specific secondary structure elements. The results are included in Figure 2 (black lines). Clearly, the calculated spectra capture the spectral shape and polarity of both the imaginary and the real experimental spectra well. The sensitivity to the peptide absolute orientation, even at a "flat" angle of 82°, becomes apparent when calculating the related spectra for the opposite molecular orientation as a reference. We have rotated the simulation box with respect to the laboratory frame by 180° by rotating the snapshot about an x-axis within the peptide layer. The spectra of the inverted snapshot (red line) match neither the calculated spectra of the simulation nor the experimental spectra.

To verify the consistency of the measured phase-resolved spectra with the related and well-known homodyne detected spectra we calculated the absolute square of the imaginary and real spectra parts and compared the results with experimental homodyne spectra and homodyne spectra calculated from the simulation. The results are summarized in Figure 2c−e. The heterodyne and homodyne spectra as well as the calculations are in excellent agreement and exhibit a peak near 1645 cm^{-1}, which agrees well with literature values.

In summary, we have determined the absolute orientation of the model peptide LKα14 at the air−water interface using a combination of phase-resolved SFG data, MD simulations, and spectra calculations. We found that the widely studied model peptide LKα14 on average adopts a rather planar orientation at water surfaces and is slightly tilted (82°) with the N-terminus

Scheme 1. Model Leucine (L) and Lysine (K) Peptides LKα14 Designed To Adopt α-Helical Secondary Structures at Interfaces[a]

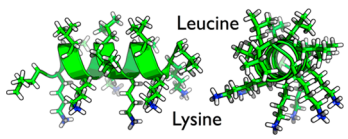

[a]LKα14 peptides are amphiphilic with hydrophobic leucines and hydrophilic lysines orienting to opposite sides of the helix.

DOI: 10.1021/acs.jpclett.7b01059
J. Phys. Chem. Lett. 2017, 8, 3101−3105

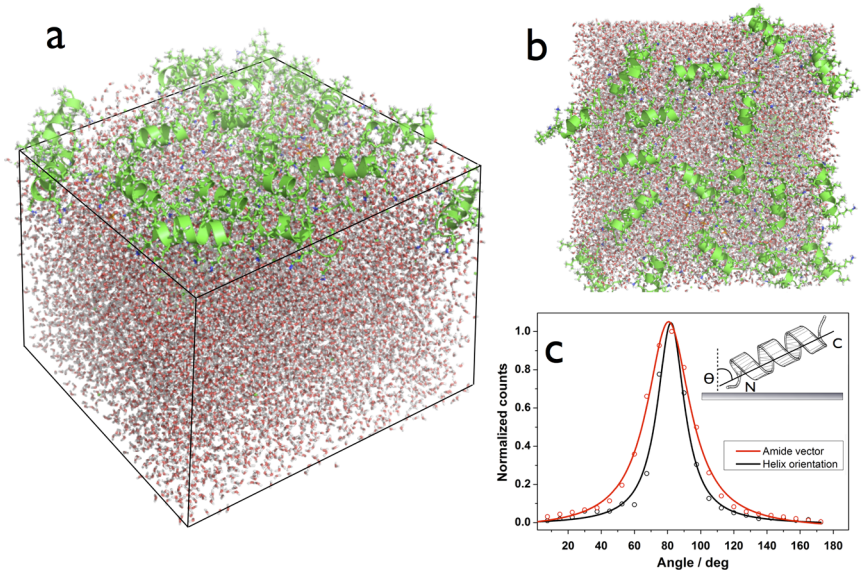

Figure 1. Snapshot of the MD simulation of LKα14 at the air−water interface at time point 100 ns: (a) side view and (b) top view of the simulation box. The LKα14 peptides predominantly assume α-helical secondary structures. While the leucine side chains are oriented away from the water surface, the lysine side chains are interacting with the water. (c) Orientation analysis of the amide-I bonds and the helix axes of the peptides.

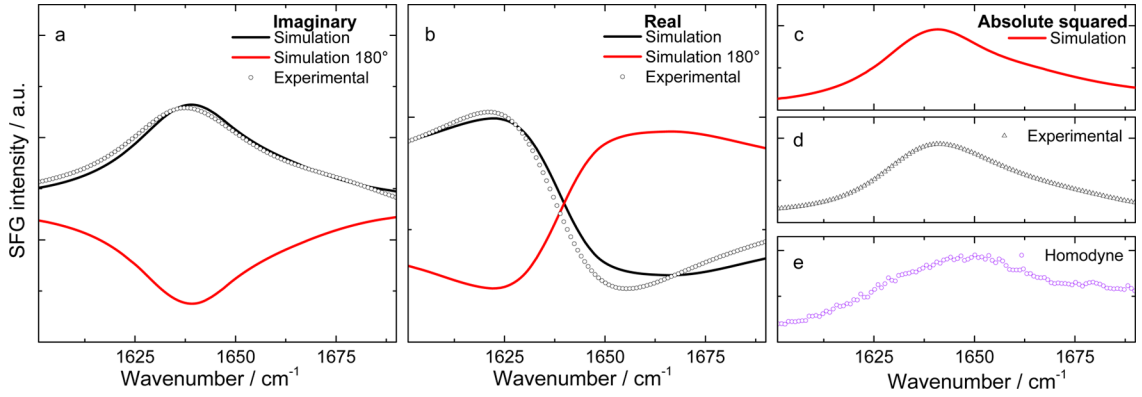

Figure 2. Experimental and theoretical SFG spectra for LKα14 at the air−water interface. (a) Experimental (dots) imaginary spectrum along spectra calculated for the MD snapshot (black) and the snapshot rotated by 180° (red). (b) Calculated real SFG spectra. (c) Absolute squared spectrum calculated from the simulation spectra. (d) Absolute squared spectrum constructed from the experimental heterodyne spectra. (e) Homodyne detected SFG spectrum as reference.

oriented towards the water phase (Scheme 2). Orientation measurements of water molecules, hydrocarbons, and protein components have been successfully used for years to answer questions in physical chemistry. Knowledge of the absolute orientation of proteins is important for protein-based biosensors, drug design, and the development of new biocompatible coatings. The procedure presented here allows direct assessment of absolute protein orientation by a comparison of simulated structures with SFG spectroscopic data.

Scheme 2. Illustration of the Average Orientation of the LK Peptides at the Air−Water Interface As Determined from the MD Simulations and Phase-Resolved SFG Experiments[a]

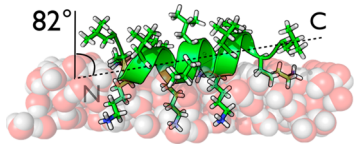

[a]The N-terminus is pointing into the water phase.

EXPERIMENTAL METHODS

Details of the phase-specific SFG setup have been described before. Briefly, a 10 mJ laser pulse with a pulse duration of 40 fs is generated by a Ti:Sa amplified laser (Spitfire Ace, centered at 800 nm). A 2 mJ portion of the amplifier output is branched out to pump an optical paramagnetic amplifier (TOPAS, Light Conversion), which generates 2 μJ broadband pulses centered at 6.1 μm with a bandwidth of roughly 300 cm^{-1}. Another 1 mJ is guided through a Fabry−Perot Etalon (SLS Optics Ltd.) to narrow the broadband 800 nm pulses to a bandwidth of 11 cm^{-1} with 3 μJ pulse energy. The IR and visible pulses are focused on a gold mirror with a 100 cm (visible) and a 5 cm (IR) focal length lens and overlapped in space and time to generate the local oscillator. Local oscillator, IR, and visible pulses are refocused to the sample using a concave mirror. The local oscillator is either delayed by a 1 mm thick fused silica plate for phase-specific heterodyne detected SFG spectra or

DOI: 10.1021/acs.jpclett.7b01059
J. Phys. Chem. Lett. 2017, 8, 3101−3105

blocked with a metal plate for homodyne detected SFG spectra. The local oscillator and the sample SFG pulses are collimated and focused to a spectrometer and finally detected by an EMCCD camera. Subsequently, the imaginary and real parts are deduced from the interference spectrum by Fourier transformation. The formalism explaining this procedure has been described in detail before.[28,38]

The spectra are calculated with an amide-I exciton model for the backbone amide groups, based on the formalism described in ref 19. Briefly, the Hamiltonian is constructed with (I) the local mode gas phase frequencies modulated by a hydrogen-bond induced red-shift on the diagonal; (II) for the nearest neighbors, a through-bond coupling model based on parametrized quantum-chemical calculations with the 6-31G+(d) basis set and B3LYP-functional that correlates the dihedral angles between the neighboring the local amide-I modes to the interaction strength;[39] and (III) for the non-nearest neighbors, the transition dipole coupling (TDC) model is used, which calculates the through-space coupling between amide groups based on their relative orientation and distance.[40] When the Hamiltonian is diagonalized, the eigenvalues and eigenmodes of the normal modes are obtained, from which the IR, Raman, and SFG responses are calculated. The heterodyned spectra can then be obtained using

$$\chi_{ijk,\mathrm{RE}} = \mathrm{Re}\left(\sum_{\nu} \frac{\chi_{ijk,\nu}\sqrt{\Gamma_{\mathrm{Exc}}+\Gamma_{\nu}}}{\omega_{\nu}+\omega-i(\Gamma_{\mathrm{Exc}}+\Gamma_{\nu})}\right)$$

$$\chi_{ijk,\mathrm{Im}} = \mathrm{Im}\left(\sum_{\nu} \frac{\chi_{ijk,\nu}\sqrt{\Gamma_{\mathrm{Exc}}+\Gamma_{\nu}}}{\omega_{\nu}+\omega-i(\Gamma_{\mathrm{Exc}}+\Gamma_{\nu})}\right)$$

with $\chi_{ijk,\nu}$, Γ_{ν}, and ω_{ν} the hyperpolarizability, line width, and frequency of normal mode ν, respectively. We assume all Γ_{ν} are 5 cm^{-1} and set Γ_{Exc}, the width of the visible pulse, to 11 cm^{-1}.

To achieve the best match between calculated and experimental data, we first determined a constant value for the nonresonant phase that was applied to all spectra. The only other fixed parameter used was an absolute intensity scaling factor for each imaginary, real, and absolute spectrum, i.e., the calculations are completely unbiased in terms of resonance position, relative intensity of the different modes, and phase.

Molecular Dynamics Simulations. Simulations were carried out using the GROMACS 4.6 simulation package.[41] Peptide parameters are defined in the AMBER99SB-ildn force field; parameters for phosphate ions were adopted from ref 5, and the TIP3P water model was used. The initial state was packed using Packmol, with 23 peptides at the vacuum−water interface of 8 × 8 × 7 nm of vacuum and 8 × 8 × 6.8 nm of water, containing 10 phosphate anions and sufficient chloride anions to neutralize the simulation box. Therefore the system can be described as 6.8 nm slabs of water separated by 7 nm of vacuum. Topology and coordinate files were generated with Tleap and subsequently converted to GROMACS-type files using Acpype. Constraining all bonds with the LINCS algorithm, the simulations were run at a 2 fs time step with periodic boundary conditions in all three dimensions for 100 ns, using the particle mesh Ewald (PME) method for long-range Coulomb interactions.[42] The distance for Lennard-Jones potential cutoff was set to 1 nm, and the temperature was maintained at 300 K using velocity rescaling with a stochastic term.[43] The tilt of the peptide chain at the vacuum−water interface was calculated using a Python implementation of a method developed by Kahn, based on the α carbon atoms along the peptide chain, disregarding the first and last two amino acids.

■ ASSOCIATED CONTENT

Supporting Information

The Supporting Information is available free of charge on the ACS Publications website at DOI: 10.1021/acs.jpclett.7b01059.

Definition of the transition diploe moments and molecular hyperpolarizability and calculation of the peptide orientations (PDF)

■ AUTHOR INFORMATION

Corresponding Author

*E-mail: weidner@chem.au.dk.

ORCID

Mischa Bonn: 0000-0001-6851-8453

Tobias Weidner: 0000-0002-7083-7004

Notes

The authors declare no competing financial interest.

■ ACKNOWLEDGMENTS

This work was supported by the Max Planck Graduate Center with the Johannes Gutenberg-Universität Mainz (MPGC). L.S. and T.W. thank the Deutsche Forschungsgemeinschaft (WE4478/4-1) for financial support. S.W. and S.J.R. thank the Netherlands Organization for Scientific Research (NWO) for financial support. We thank Dr. Ellen Backus for helpful discussions.

■ REFERENCES

(1) Lu, H.; Hood, M. A.; Mauri, S.; Baio, J. E.; Bonn, M.; Munoz-Espi, R.; Weidner, T. Biomimetic Vaterite Formation at Surfaces Structurally Templated by Oligo(Glutamic Acid) Peptides. *Chem. Commun.* **2015**, *51*, 15902−15905.

(2) Ding, B.; Jasensky, J.; Li, Y. X.; Chen, Z. Engineering and Characterization of Peptides and Proteins at Surfaces and Interfaces: A Case Study in Surface-Sensitive Vibrational Spectroscopy. *Acc. Chem. Res.* **2016**, *49*, 1149−1157.

(3) Yin, H.; Flynn, A. D. Drugging Membrane Protein Interactions. *Annu. Rev. Biomed. Eng.* **2016**, *18*, 51−76.

(4) Brady, D.; Jordaan, J. Advances in Enzyme Immobilisation. *Biotechnol. Lett.* **2009**, *31*, 1639−1650.

(5) Lutz, H.; Jaeger, V.; Berger, R.; Bonn, M.; Pfaendtner, J.; Weidner, T. Biomimetic Growth of Ultrathin Silica Sheets Using Artificial Amphiphilic Peptides. *Adv. Mater. Interfaces* **2015**, *2*, 1500282.

(6) Rossier, J. S.; Girault, H. H. Enzyme Linked Immunosorbent Assay on a Microchip with Electrochemical Detection. *Lab Chip* **2001**, *1*, 153−157.

(7) Castner, D. G. Surface Science: View from the Edge. *Nature* **2003**, *422*, 129−130.

(8) Baio, J. E.; Weidner, T.; Ramey, D.; Pruzinsky, L.; Castner, D. G. Probing the Orientation of Electrostatically Immobilized Cytochrome C by Time of Flight Secondary Ion Mass Spectrometry and Sum Frequency Generation Spectroscopy. *Biointerphases* **2013**, *8*, 18.

(9) Strandberg, E.; Wadhwani, P.; Tremouilhac, P.; Dürr, U. H. N.; Ulrich, A. S. Solid-State Nmr Analysis of the Pgla Peptide Orientation in Dmpc Bilayers: Structural Fidelity of 2h-Labels Versus High Sensitivity of 19f-Nmr. *Biophys. J.* **2006**, *90*, 1676−1686.

(10) Stevens, M. A.; McKay, J. E.; Robinson, J. L. S.; El Mkami, H.; Smith, G. M.; Norman, D. G. The Use of the Rx Spin Label in Orientation Measurement on Proteins, by Epr. *Phys. Chem. Chem. Phys.* **2016**, *18*, 5799−5806.

DOI: 10.1021/acs.jpclett.7b01059
J. Phys. Chem. Lett. 2017, 8, 3101−3105

(11) Hennig, R. IM30 Triggers Membrane Fusion in Cyanobacteria and Chloroplasts. *Nat. Commun.* **2015**, *6*, 7018.
(12) Bellucci, L.; Ardevol, A.; Parrinello, M.; Lutz, H.; Lu, H.; Weidner, T.; Corni, T. The Interaction with a Gold Surface Suppresses Fiber-Like Conformations of the Amyloid Aβ16−22 Peptide. *Nanoscale* **2016**, *8*, 8737−8748.
(13) Ye, S.; Li, H.; Yang, W.; Luo, Y. Accurate Determination of Interfacial Protein Secondary Structure by Combining Interfacial-Sensitive Amide I and Amide Iii Spectral Signals. *J. Am. Chem. Soc.* **2014**, *136*, 1206−1209.
(14) Shen, Y. R. *The Principles of Nonlinear Optics*, 1st ed.; John Wiley & Sons: New York, 1984.
(15) Zhang, C.; Myers, J. N.; Chen, Z. Elucidation of Molecular Structures at Buried Polymer Interfaces and Biological Interfaces Using Sum Frequency Generation Vibrational Spectroscopy. *Soft Matter* **2013**, *9*, 4738−4761.
(16) Weidner, T.; Castner, D. G. Sfg Analysis of Surface Bound Proteins: A Route Towards Structure Determination. *Phys. Chem. Chem. Phys.* **2013**, *15*, 12516−24.
(17) Baio, J. E.; Zane, A.; Jaeger, V.; Roehrich, A. M.; Lutz, H.; Pfaendtner, J.; Drobny, G. P.; Weidner, T. Diatom Mimics: Directing the Formation of Biosilica Nanoparticles by Controlled Folding of Lysine-Leucine Peptides. *J. Am. Chem. Soc.* **2014**, *136*, 15134−7.
(18) Ding, B.; Panahi, A.; Ho, J. J.; Laaser, J. E.; Brooks, C. L.; Zanni, M. T.; Chen, Z. Probing Site-Specific Structural Information of Peptides at Model Membrane Interface in Situ. *J. Am. Chem. Soc.* **2015**, *137*, 10190−10198.
(19) Roeters, S. J.; van Dijk, C. N.; Torres-Knoop, A.; Backus, E. H.; Campen, R. K.; Bonn, M.; Woutersen, S. Determining In Situ Protein Conformation and Orientation from the Amide-I Sum-Frequency Generation Spectrum: Theory and Experiment. *J. Phys. Chem. A* **2013**, *117*, 6311−22.
(20) Nguyen, K. T.; Le Clair, S. V.; Ye, S. J.; Chen, Z. Orientation Determination of Protein Helical Secondary Structures Using Linear and Nonlinear Vibrational Spectroscopy. *J. Phys. Chem. B* **2009**, *113*, 12169−12180.
(21) Nguyen, K. T.; King, J. T.; Chen, Z. Orientation Determination of Interfacial Beta-Sheet Structures in Situ. *J. Phys. Chem. B* **2010**, *114*, 8291−8300.
(22) Lotze, S.; Versluis, J.; Olijve, L. L.; van Schijndel, L.; Milroy, L. G.; Voets, I. K.; Bakker, H. J. Communication: Probing the Absolute Configuration of Chiral Molecules at Aqueous Interfaces. *J. Chem. Phys.* **2015**, *143*, 201101.
(23) Strazdaite, S.; Meister, K.; Bakker, H. J. Orientation of Polar Molecules near Charged Protein Interfaces. *Phys. Chem. Chem. Phys.* **2016**, *18*, 7414−8.
(24) Okuno, M.; Ishibashi, T.-a. Heterodyne-Detected Achiral and Chiral Vibrational Sum Frequency Generation of Proteins at Air/Water Interface. *J. Phys. Chem. C* **2015**, *119*, 9947−9954.
(25) Okuno, M.; Ishibashi, T. A. Chirality Discriminated by Heterodyne-Detected Vibrational Sum Frequency Generation. *J. Phys. Chem. Lett.* **2014**, *5*, 2874−8.
(26) Ostroverkhov, V.; Waychunas, G. A.; Shen, Y. R. New Information on Water Interfacial Structure Revealed by Phase-Sensitive Surface Spectroscopy. *Phys. Rev. Lett.* **2005**, *94*, 046102.
(27) Pool, R. E.; Versluis, J.; Backus, E. H. G.; Bonn, M. Comparative Study of Direct and Phase-Specific Vibrational Sum-Frequency Generation Spectroscopy: Advantages and Limitations. *J. Phys. Chem. B* **2011**, *115*, 15362−15369.
(28) Nihonyanagi, S.; Yamaguchi, S.; Tahara, T. Direct Evidence for Orientational Flip-Flop of Water Molecules at Charged Interfaces: A Heterodyne-Detected Vibrational Sum Frequency Generation Study. *J. Chem. Phys.* **2009**, *130*, 204704.
(29) Stiopkin, I. V.; Jayathilake, H. D.; Bordenyuk, A. N.; Benderskii, A. V. Heterodyne-Detected Vibrational Sum Frequency Generation Spectroscopy. *J. Am. Chem. Soc.* **2008**, *130*, 2271−2275.
(30) Degrado, W. F.; Wasserman, Z. R.; Lear, J. D. Protein Design, a Minimalist Approach. *Science* **1989**, *243*, 622−628.
(31) Degrado, W. F.; Lear, J. D. Induction of Peptide Conformation at Apolar Water Interfaces 0.1. A Study with Model Peptides of Defined Hydrophobic Periodicity. *J. Am. Chem. Soc.* **1985**, *107*, 7684−7689.
(32) Weidner, T.; Apte, J. S.; Gamble, L. J.; Castner, D. G. Probing the Orientation and Conformation of Alpha-Helix and Beta-Strand Model Peptides on Self-Assembled Monolayers Using Sum Frequency Generation and Nexafs Spectroscopy. *Langmuir* **2010**, *26*, 3433−3440.
(33) Weidner, T.; Breen, N. F.; Li, K.; Drobny, G. P.; Castner, D. G. Sum Frequency Generation and Solid-State Nmr Study of the Structure, Orientation, and Dynamics of Polystyrene-Adsorbed Peptides. *Proc. Natl. Acad. Sci. U. S. A.* **2010**, *107*, 13288−13293.
(34) Engin, O.; Sayar, M. Adsorption, Folding, and Packing of an Amphiphilic Peptide at the Air/Water Interface. *J. Phys. Chem. B* **2012**, *116*, 2198−207.
(35) Dalgicdir, C.; Sayar, M. Conformation and Aggregation of Lkalpha14 Peptide in Bulk Water and at the Air/Water Interface. *J. Phys. Chem. B* **2015**, *119*, 15164−75.
(36) Deighan, M.; Pfaendtner, J. Exhaustively Sampling Peptide Adsorption with Metadynamics. *Langmuir* **2013**, *29*, 7999−8009.
(37) Sprenger, K. G.; He, Y.; Pfaendtner, J. Probing How Defects in Self-Assembled Monolayers Affect Peptide Adsorption with Molecular Simulation. *Mol. Model. Simul.* **2016**, 21−35.
(38) Hsieh, C. S.; Okuno, M.; Hunger, J.; Backus, E. H. G.; Nagata, Y.; Bonn, M. Aqueous Heterogeneity at the Air/Water Interface Revealed by 2d-Hd-Sfg Spectroscopy. *Angew. Chem., Int. Ed.* **2014**, *53*, 8146−8149.
(39) Gorbunov, R.; Kosov, D.; Stock, G. Ab Initio-Based Exciton Model of Amide I Vibrations in Peptides: Definition, Conformational Dependence, and Transferability. *J. Chem. Phys.* **2005**, *122*, 224904.
(40) Krimm, S.; Abe, Y. Intermolecular Interaction Effects in the Amide I Vibrations of B Polypeptides. *Proc. Natl. Acad. Sci. U. S. A.* **1972**, *69*, 2788−2792.
(41) Hess, B. P-Lincs: A Parallel Linear Constraint Solver for Molecular Simulation. *J. Chem. Theory Comput.* **2008**, *4*, 116−122.
(42) Darden, T.; York, D.; Pedersen, L. Particle Mesh Ewald - an N.Log(N) Method for Ewald Sums in Large Systems. *J. Chem. Phys.* **1993**, *98*, 10089−10092.
(43) Bussi, G.; Donadio, D.; Parrinello, M. Canonical Sampling through Velocity Rescaling. *J. Chem. Phys.* **2007**, *126*, 014101.

DOI: 10.1021/acs.jpclett.7b01059
J. Phys. Chem. Lett. 2017, 8, 3101−3105